Deng Yuzhe CID: 06047882, Liu Xinqi CID: 06050480 Cai Hongzhe CID: 06055169, Xu Jiahan CID: 06047124

Temperature Sensor Report

1. Introduction

This report presents the design and implementation of customized readout circuits for four different types of temperature sensors: RTD, NTC, Thermocouple, and Digital Sensor. Each sensor was characterized over a temperature range of 0 °C to 100 °C, and its performance was evaluated in terms of response time, accuracy, stability and linearity. The strengths and limitations of each sensor for different application scenarios are shown by comparing their practical performance under the same test conditions.

2. Design and Analysis of Test Bed

1) Testbed Setup Overview

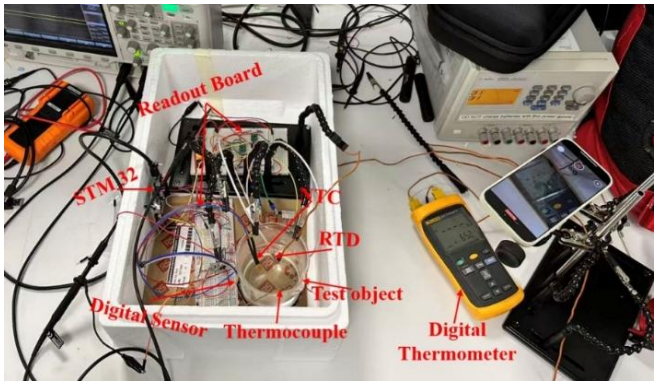

Figure 1 Physical Setup

To ensure controlled and repeatable temperature characterization, all sensors, the readout circuits, and the water-filled beaker (test object) were placed inside a Styrofoam box with a lid, providing effective thermal insulation. The STM32 microcontroller was used to acquire sensor outputs: the RTD and NTC sensors were interfaced through the analogue readout boards and sampled using the ADC, while the digital sensor and the thermocouple were read directly via GPIO inputs. A digital fluke thermometer served as the reference instrument for verifying measurement accuracy. Figure 1 shows the physical setup, and Figure 2 illustrates the complete system block diagram.

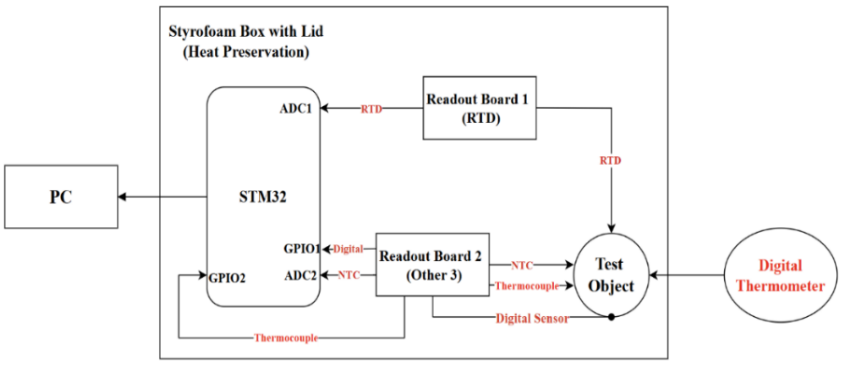

Figure 2 Complete System Block Diagram

2) Thermal Conditioning and Measurement Challenges

Water was selected as the measurement medium due to its high thermal capacity, stability, and relatively uniform temperature distribution around the sensors. For heating, boiling water was mixed with a small amount of 25 °C water, and a maximum temperature of 92 °C was used inside the insulated box. For cooling, a mixture of ice and a small volume of warm water was applied, enabling rapid initial cooling followed by slower cooling as the ice melted. This produced a usable range of

$6 - 92\ °C,$ sufficient to evaluate all four sensors while remaining relatively safe.

This heating–cooling approach also introduced limitations. During heating, convection and bottom-up warming can reduce heat transfer to partially submerged sensors. During cooling, ice may create local cold spots, causing unrealistically low readings for sensors near the ice. In addition, the digital sensor and NTC could not be fully submerged, which increased measurement instability, especially given their fast response to temperature changes.

3) Safety Considerations

Safety was prioritised overreaching extreme temperature regions; therefore, the operating range was intentionally limited to approximately $6 - 92\ °C$. Key risks, such as the heat tolerance of the Styrofoam box, splashing onto nearby electronics, potential glass-beaker fracture under rapid temperature changes, and humidity buildup, were identified in advance. To mitigate these hazards, a cardboard insulation layer was placed beneath the beaker, electronic boards were elevated and kept at a safe distance from the water container, cables were secured to avoid accidental tipping, and temperature transitions were applied gradually. The enclosure was briefly opened after heating cycles to release moisture. With these precautions, the setup remained safe while still providing a wide and repeatable temperature range for sensor evaluation.

4) Strength and Weakness of Setup

The setup offered several strengths for controlled temperature testing: the insulated enclosure reduced convective heat loss, water provided stable thermal conditions, and fixed probe mounting ensured consistent immersion depth and repeatable thermal contact. These features reduced test-to-test variation and improved consistency. However, limitations were also recognised. Hot water-driven heating can create temperature difference between top and bottom of the beaker, ice-assisted cooling may produce local cold spots, and humidity can accumulate during heating cycles. The glass beaker and Styrofoam box also set practical safety limits on the temperature range. These constraints do not invalidate the results but are considered when interpreting sensor performance.

3. Design of Readout Circuit & Sensor Characterisation

3.1 Thermistor (NTC)

3.1.1 NTC Thermistor Characterization

NTC thermistor exhibits an exponential decrease in resistance with temperature using the β-parameter model in equation (1):

$$R_{NTC} = R_0 e^{\beta[1+\gamma(T_m - T_0)](\frac{1}{T_m} - \frac{1}{T_0})} \quad (1)$$

where R_0 is the resistance at T_0 = 25 °C, T_m is the measured temperature, β is a material dependent constant.

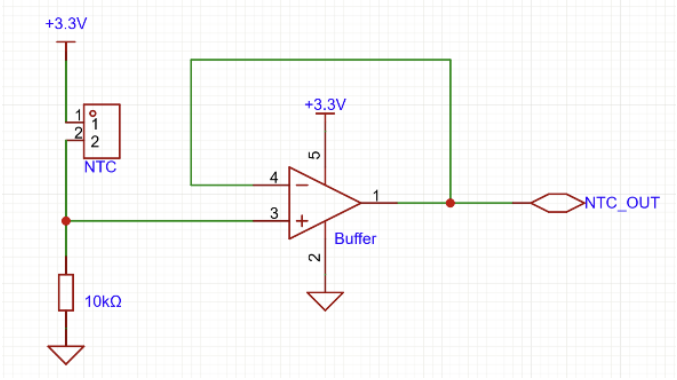

Figure 3 NTC Readout Circuit

Regarding the readout Circuit of $10\ k\Omega$ NTC, voltage-divider configuration with a fixed $10\ k\Omega$ resistor is applied in Figure 3 and equation (2):

$$V_{out} = 3.3\ \text{V} \cdot \frac{10k}{R_{NTC}+10k} \tag{2}$$

3.1.2 Experimental Results & Discussion

In Figure 4, the NTC provides good sensitivity, the accuracy is constrained by the thermal setup, due to the thermistor could not be fully immersed in water.

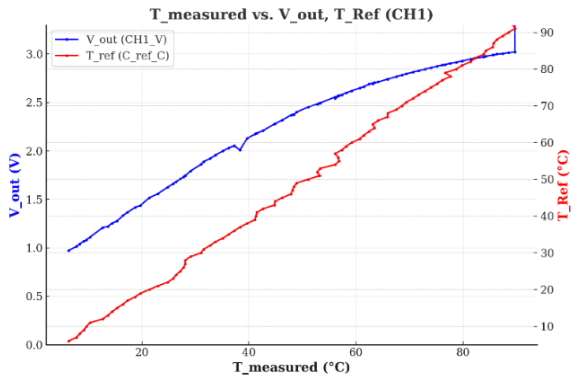

Figure 4 Results of NTC

Accuracy: The NTC accuracy was evaluated by comparison with a Fluke digital thermometer taken as the reference T_{ref}. Agreement is good in the mid-range, while deviations increase near $6\ °C\ and\ 92\ °C$ due to the intrinsic nonlinearity of the NTC and limited calibration. Accuracy is mainly limited by sensor nonlinearity, reference uncertainty, and thermal coupling.

Precision: Each data point is averaged over multiple samples. Precision is generally good, though increased jitter is observed in the high-sensitivity region. This fluctuation is dominated by environmental thermal instability rather than ADC quantization or electronic noise.

Sensitivity and Linearity: The NTC shows high sensitivity at low-to-mid temperatures, decreasing toward the upper range. The voltage–temperature relationship is strongly nonlinear, as expected. Single-point calibration is therefore insufficient over $6\ °C - 92\ °C$, and linearization is required for improved accuracy (By LPA).

Response Time: The NTC reaches final value using about 2 s during heating ($6\ °C \rightarrow 76\ °C$) and cooling ($76\ °C \rightarrow 6\ °C$). This fast response is typical of small-bead NTC thermistors and is limited by thermal mass and heat transfer.

Hysteresis: A small hysteresis is observed between heating and cooling curves. This effect originates from asymmetric heat-transfer conditions during heating and cooling, not from the NTC or readout circuit.

Stability: Under static conditions, the NTC output is stable. Under dynamic temperature changes, convection and partial immersion introduce ripple output and small drift. Overall, the NTC offers high sensitivity and fast response, but accuracy and stability depend strongly on calibration and mechanical setup.

3.2 RTD

3.2.1 RTD Characterization and Circuit Operation

For a standard Pt1000, it is often sufficient to use the linear approximation in the range relevant

to this work (approximately $0 - 100°C$):

$$R(T) \approx 1000 \cdot (1 + 0.00385 \cdot T) \tag{3}$$

where $R(T)$ is the RTD resistance at temperature T in ℃, $R_0 = 1000\Omega$, is the resistance at $0°C$, and $\alpha \approx 0.00385/℃$, is the temperature coefficient of resistance.

Through Figure 4, the RTD circuit is mainly divided into three parts. First, the Wheatstone bridge generates the left and right mid-point voltages, which correspond to V_+ and V_- in Equation (3). These two nodes are then fed into unity-gain buffers. The purpose of the buffers is to present a very high input impedance, so they do not disturb the operation of the bridge, while at the same time providing low-impedance outputs. Finally, the buffered signals are applied to a differential amplifier. This stage rejects the common-mode component and provides gain (≈ 10) for V_{out}. The following equation shows the relationship between ΔR and V_{out}.

$$V_{out}(T) = 10 \cdot (V_+ - V_-) = 10 \cdot V_{in}\left(\frac{1}{2} - \frac{R_5}{R_{RTD}(T) + R_5}\right)$$
$$= 10 \cdot V_{in} \cdot \frac{\Delta R(T)}{4000 + 2\Delta R(T)} \approx k_R\, \Delta R(T) \tag{4}$$

where $\Delta R(T) = R_{RTD}(T) - R_5$ and k_R is a constant, set by the bridge and V_{in}. As a result, the small resistance-induced imbalance of the bridge is converted into output voltage that is approximately proportional to temperature over the $0 - 100$ ℃ range; the exact slope and offset of this transfer are determined experimentally in the calibration and results sections.

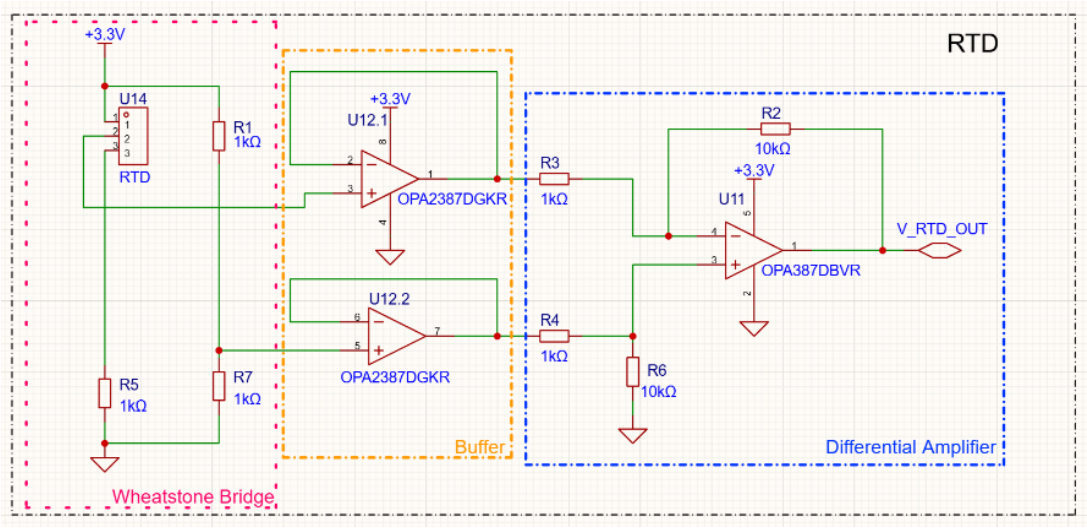

Figure 5 The circuit diagram of RTD

3.2.2 Experimental Results & Discussion

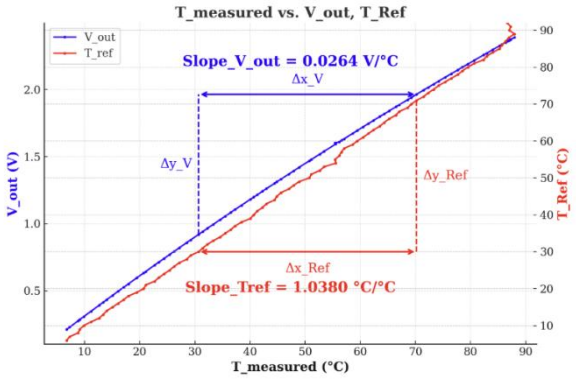

Figure 6 The result of RTD

Accuracy: The RTD accuracy was evaluated by comparing the calibrated RTD temperature with a digital thermometer taken as the reference T_{ref}. The red line in Fig. 6 shows T_{ref} versus the calibrated RTD temperature, its fitted slope is very close to 1, and the residual error is about $\pm 0.7°C$ over 6°C–92°C. Measurement accuracy is fundamentally limited by the reference thermometer's precision and thermal coupling quality. Errors stem from external factors like reference drift and bath gradients, as well as internal circuit offsets (bridge/op amp) which require calibration.

Precision: Each data point averages multiple RTD readings. The tight spread confirms good precision, though it is ultimately limited by electronic noise (ADC/amp) and minor physical fluctuations in the water bath. Essentially, the observed precision reflects both the readout limitations and the actual thermal stability.

Sensitivity and Linearity: The linear fit shows a sensitivity of ~0.0264 V/°C, which matches the expected bridge gain. Fig. 6 confirms the response is linear across the range. However, this linearity depends on a stable supply. While effects like self-heating or resistor drift are negligible at this scale in this design.

Response Time: The RTD takes roughly 22s to reach ≈ 90% stability between 6°C and 76°C. This lag is due to physical thermal mass, not the electronics. As seen in the top right of Fig. 6, this slow response introduces non-linearities (or oscillations), while the DAQ sampling limits slightly blur the exact transient shape.

Hysteresis: Heating and cooling curves match closely, confirming negligible hysteresis. Small deviations at high temperatures are due to thermal gradients in the bath rather than the RTD or amplifiers. This is a setup limitation where the error comes from water, not the electronics.

Stability: Unlike the rapid cooling observed at high temperatures, the water cools very slowly in the lower temperature range. This stable window can be used to verify performance, where V_{out} showed minimal fluctuation. This confirms short-term stability, assuming bath and component drift remained constant.

3.3 Thermocouple

3.3.1 Thermocouple Characterization

Type K thermocouple (Nickel-Chromium/Nickel-Alumel) is based on the Seeback Effect: When two different metals form a closed circuit and a temperature difference is created at their ends, a small electromotive force is generated in the circuit.

$$V_{TC} = S(T_{hot} - T_{cold}) \tag{5}$$

For type K thermocouples, the output voltage is approximately 41 μV/°C.

Thermocouple Amplifier MAX31855 breakout board is used for Amplifier, providing cold junction reference and ADC.

$$T_{hot} = T_{TC} + T_{cold\ sensor} \tag{6}$$

The processed temperature data are transmitted to the STM32 via an SPI interface and read through the GPIO pins.

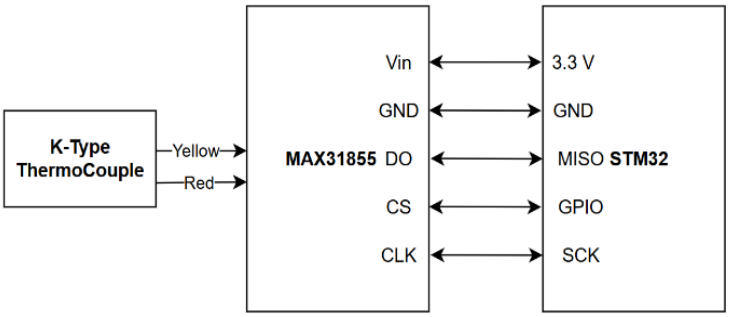

Figure 7 Connection of Thermocouple and Amplifier

Limitation: However, MAX31855 must be placed at room temperature and away from any heat source, as changes of internal temperature will cause significant errors on readout. Therefore, its location requires extra attention during circuit setup.

3.3.2 Experimental Results & Discussion

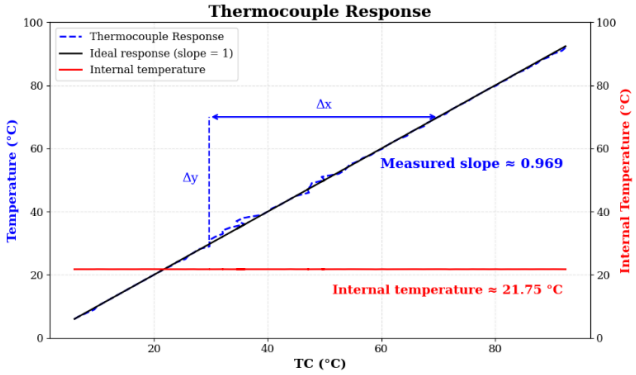

Figure 8 Thermocouple Response

The amplifier must be put away from the measurement area and placed in room temperature to provide a stable internal temperature.

Sensitivity and Linearity: As shown in Figure 8, the thermocouple and amplifier exhibit an almost perfectly linear relationship between its indicated temperature and the reference thermometer reading. Its response characteristics remain almost constant across the range, in contrast to the strongly temperature-dependent sensitivity of the NTC. This near-unity slope represented by the C_{ref} vs C_{TC} curve shows the sensitivity. As the sensitivity is almost 1 it directly shows the temperature without any calculation or readout circuit.

Stability: Measured by keeping the water in a stable temperature, its output exhibits no drift over extended periods, demonstrating exceptional stability.

Resolution: As the voltage change caused by the Seeback effect is very small, the resolution of a thermocouple depends primarily on the performance of its amplifier, which is $0.25°C$ of MAX31855.

Accuracy: Accuracy was assessed by comparing the thermocouple reading with the reference thermometer. The two traces agree closely across the full range, The errors are within $\pm 2°C$, in accordance with the data sheet.

Response time: Characterised by applying a step-like temperature change. The thermocouple

reached $90\ \%$ of its final value in less than 1 s for both heating and cooling, indicating a very small thermal time constant typical of fine-wire junctions with low thermal mass and good thermal contact to the medium.

Hysteresis: No significant thermal hysteresis was observed between heating and cooling curves, confirming that the junction and wiring do not store appreciable heat.

3.4 Digital Temperature Sensor

3.4.1 Digital Temperature Sensor Characterization

The DS18B20 is a fully digital temperature sensor that outputs temperature via a 1-Wire interface, so no analogue signal conditioning ($divider/amplifier/ADC$) is required. In the readout circuit (Figure 9), the sensor is connected to an STM32 GPIO with a pull-up resistor, and temperature is obtained by digital conversion and data transfer.

3.4.2 Experimental Results & Discussion

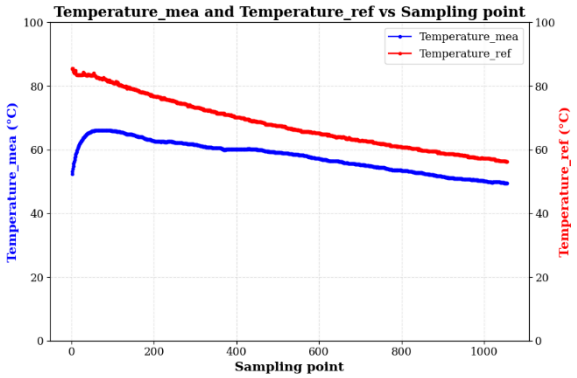

Figure 9 Digital Temperature Sensor Response

Accuracy: Accuracy is mainly limited by thermal contact to the reference T_{ref}. When thermal coupling is good (e.g., short-term immersion), agreement is reasonable; deviations increase when contact resistance is uncontrolled. Since a non-waterproof DS18B20 was used, long-term immersion can cause leakage/oxidation/electrolysis, so accuracy cannot be guaranteed under extended wet or high-temperature conditions.

Precision: Short-term repeatability is generally good after thermal stabilization, consistent with the device being factory-calibrated and digitally quantized.

Sensitivity & Linearity: Sensitivity is set by resolution. In 12-bit mode, the output step is $0.0625\ °C/LSB$ over $-55\ °C$ to $125\ °C$. The temperature response is effectively linear across the operating range due to on-chip calibration and compensation.

Response Time: The datasheet conversion time is $\sim 750\ ms$ at 12-bit resolution, while the observed response is $\sim 1-2\ s$, dominated by packaging thermal mass and heat-transfer conditions rather than the internal conversion.

Hysteresis: Intrinsic hysteresis is negligible; any observed offset between heating/cooling is attributed to thermal lag and asymmetric heat paths.

Stability: Under static ambient conditions the readings are stable, but occasional $\sim 1\ °C$ jumps were observed, likely due to system-level factors (1-Wire timing robustness, pull-up choice, incomplete conversions, supply noise, or airflow) rather than inherent sensor drift.

5) Output Collection & Signal Processing

To ensure that temperature readings are not affected by differences in sampling time, all sensors were sampled synchronously with a fixed acquisition interval of 1 second. The collected data were further processed using filtering and averaging functions to suppress noise and ensure a smooth temperature output. The applied filtering slightly reduces the temporal responsiveness of the system, resulting in a small increase in the measured response time.

By adopting this unified sampling and processing strategy, all types of temperature sensors share a common time reference and a consistent output format. This approach enables the extraction of key performance metrics, including accuracy, precision, linearity, response time, hysteresis, and stability, and allows for a fair comparison of these metrics among different sensors in subsequent sections.

6) Temperature Sensor & Output Comparison

Table 1 Characteristics Comparison of 4 kinds of Temperature Sensors

Aspect	NTC	RTD (Pt1000)	Digital Sensor	Thermocouple
Temperature range	Narrow–medium ($\approx -30\ to\ 125\ °C$)	Medium ($\approx -50\ to\ 280\ °C$)	Limited by IC ($typ.\ -55\ to\ 125\ °C$)	Very wide ($good\ up\ to\ 500\ °C$)
Sensitivity	High, strongly non-linear	Low, almost linear	Fixed internal resolution (e.g. 0.0625 °C)	Low (µV/°C), needs high-gain readout
Linearity	Poor, requires look-up / curve fit	Fair linear	Excellent (factory linearized)	Moderate
Accuracy (in our setup)	placement-dependent	High, ≈ ±0.7 °C after calibration	High, ± 0.5°C Accuracy from -10°C to +85°C	Good relative accuracy
Response time (in our setup)	Fast (2s)	Slow (22s)	Fast (less than 1s)	Fast to Slow
Self-heating	Significant if current too high	Present but small with low-current excitation	Negligible	Negligible
Circuit complexity	Simple divider / bridge + ADC	Bridge + buffer + differential amplifier	Very simple (digital interface only)	Needs instrumentation amp / cold-junction IC
Calibration effort	High (non-linear R–T curve)	Moderate (offset + gain correction)	Very low (factory calibrated)	Moderate–high (CJC + polynomial fit)
Cost	Very low ($0.95)	High wire wound ($11.95)	Medium ($3.95)	High ($9.95)
Specific Applications	Consumer electronics	Accurate industrial / lab measurement	Consumer/embedded devices IoT devices	Furnaces and engines

According to the experiment:
RTD stands out for absolute accuracy, but it is the slowest. After calibration, the RTD shows the tightest agreement with the reference, with a residual error of about $\pm 0.7\ °C$ over $6 - 92\ °C$. However, it is also the slowest in transients: the measured $t_{0.9} \approx 22\ s\ (6 \rightarrow 76\ °C)$ can be explained by the probe's high thermal mass (stainless-steel sheath and fillers acting as a thermal buffer), which is consistent with the lag or oscillation seen during fast temperature changes.

Thermocouple with the amplifier stands out for speed and stability—but only if the cold junction stays stable. In the step test it reaches ≈ 90% in <1 s (heating and cooling), far faster than the sheathed probe sensors, indicating a very small thermal time constant (fine junction + good contact). Its accuracy in this setup stays within ±2 °C, and it shows no drift in stable-water conditions.

NTC has the strongest nonlinearity (and placement sensitivity). Good mid-range agreement can be seen but noticeably larger deviations near ~6 °C and ~92 °C, which the links directly to the NTC's intrinsic nonlinear R–T characteristic and limited calibration, plus the practical issue that it could not be fully immersed, making thermal coupling less controlled. This same "small bead + fast thermal response" explains why it reacts quickly (≈ 2 s to 90% on heating) yet also exhibits more ripple and drift under dynamic conditions when convection/partial immersion vary.

DS18B20 has the advantage of plug-and-play linearised output, but the experiment shows occasional digital jumps and contact-limited accuracy. Its effective sensitivity is set by quantisation (12-bit 0.0625 °C/LSB), and the observed response (~1–2 s) is dominated by packaging/heat transfer rather than conversion time (~750 ms). Measurement shows that accuracy degrades when thermal contact is not well controlled, and occasional ~1 °C jumps are as system-level effects (1-Wire robustness, pull-up, incomplete conversions, supply noise, airflow). The limitation is amplified here because a non-waterproof DS18B20 was used, so long immersion can introduce leakage/oxidation/electrolysis and make readings less trustworthy.

7) Readout System Implementation & Challenges

7.1 Suitability of the Readout Electronics for Each Sensor Type

For the RTD, a Wheatstone bridge, unity-gain buffers, and a differential amplifier feeding the ADC form an appropriate interface to its resistance-based sensing principle. The circuit provides high input impedance and sufficient gain, and—after offset calibration—delivers a nearly linear, high-SNR voltage proportional to temperature. For the NTC, a similar resistive readout with analogue amplification is also suitable, provided that the non-linear $R(T)$ curve is corrected by calibration or lookup tables. The digital temperature sensor integrates its own ADC and linearisation, so the external readout is essentially limited to a digital bus interface, which is intrinsically well matched to this sensor type. For the thermocouple, a low-noise differential amplifier and ADC are in principle appropriate for the μV-level thermoelectric signal, but performance is more sensitive to PCB layout and reference-junction handling than for RTD/NTC.

7.2 Consideration of Self-Heating, Thermoelectric Voltages, SNR, and Loading

Self-heating and loading were explicitly considered for the resistive sensors. The RTD and NTC bias currents were chosen low enough that Joule heating remains negligible ($< 0.1°C$) compared with the target accuracy, while the amplifier inputs present a very high impedance so that electrical loading is insignificant. For thermocouples, the dominant challenge is cold-junction temperature stability rather than self-heating. External thermal sources and temperature gradients along the wiring can generate μV-level offsets comparable to the useful signal. Therefore, the cold junction should be placed away from thermal disturbances and maintained at a stable, well-defined temperature, either through environmental control or cold-junction compensation. SNR is high for the amplified RTD and NTC outputs, ADC input-referred noise is negligible, and quantization becomes the dominant limitation. In contrast, the thermocouple's minute signal requires high gain and careful filtering

(particularly against 50/60 Hz mains hum) to avoid noise-limited performance which are realized by MAX31855.

7.3 Interfacing and Correctness of Data Acquisition (Digitalisation Error)

The analogue interfacing for RTD and NTC uses precision resistors, rail-to-rail op-amps, and a shared ADC channel, which is appropriate from both an electrical and measurement-range perspective. Resistor mismatch in the RTD bridge and gain network produced a noticeable DC offset at the amplifier output; this was corrected by applying a 0.093 V analogue offset and a further $9\,mV$ digital correction to V_{out} during ADC processing. For the NTC, an additional digital correction of about 2 mV was applied to compensate for ADC reading errors. These explicit corrections show that digitisation errors (offset and gain) were identified and mitigated rather than ignored. For the digital temperature sensor, the serial interface eliminates external ADC errors, so correctness is mainly determined by protocol integrity and the sensor's own datasheet specifications. For the thermocouple, the amplifier–ADC chain provides adequate resolution, but the overall accuracy is limited more by cold-junction compensation and parasitic thermal EMFs than by the nominal ADC performance.

7.4 Cost and Efficiency of the Chosen Approach

All four sensor options used in this work are relatively inexpensive in absolute terms: the NTC is very low cost ($\approx \$0.95$), the RTD is more expensive but still affordable even in wire-wound form ($\approx \$11.95$), the digital sensor is in the medium range ($\approx \$3.95$), and the thermocouple assembly is also moderate in price ($\approx \$9.95$). As a result, cost did not dominate the design trade-offs; instead, the emphasis was on making efficient use of a common set of readout electronics. RTD and NTC share the same type of analogue front-end and ADC channels, which simplifies the hardware and reduces overall system cost per channel. The digital sensor reuses the existing microcontroller interface with almost no additional analogue components, giving good "engineering efficiency" for slightly higher device cost. The thermocouple reuses the same ADC infrastructure with a different gain setting, avoiding the need for a dedicated, more expensive thermocouple module. Overall, the chosen implementations achieve the required performance with low to moderate component cost and efficient reuse of the same readout platform across all sensor types.